

ORIGINAL ARTICLE

# The mouse liver displays daily rhythms in the metabolism of phospholipids and in the activity of lipid synthesizing enzymes

Lucas D. Gorné<sup>1</sup>, Victoria A. Acosta-Rodríguez<sup>1</sup>, Susana J. Pasquaré<sup>2</sup>, Gabriela A. Salvador<sup>2</sup>, Norma M. Giusto<sup>2</sup>, and Mario Eduardo Guido<sup>1</sup>

<sup>1</sup>*Departamento de Química Biológica, Facultad de Ciencias Químicas, CIQUIBIC-CONICET, Universidad Nacional de Córdoba, Córdoba, Argentina and* <sup>2</sup>*INIBIBB-CONICET, Universidad Nacional del Sur, Bahía Blanca, Argentina*

The circadian system involves central and peripheral oscillators regulating temporally biochemical processes including lipid metabolism; their disruption leads to severe metabolic diseases (obesity, diabetes, etc). Here, we investigated the temporal regulation of glycerophospholipid (GPL) synthesis in mouse liver, a well-known peripheral oscillator. Mice were synchronized to a 12:12 h light–dark (LD) cycle and then released to constant darkness with food *ad libitum*. Livers collected at different times exhibited a daily rhythmicity in some individual GPL content with highest levels during the subjective day. The activity of GPL-synthesizing/remodeling enzymes: phosphatidate phosphohydrolase 1 (PAP-1/lipin) and lysophospholipid acyltransferases (LPLATs) also displayed significant variations, with higher levels during the subjective day and at dusk. We evaluated the temporal regulation of expression and activity of phosphatidylcholine (PC) synthesizing enzymes. PC is mainly synthesized through the Kennedy pathway with Choline Kinase (ChoK) as a key regulatory enzyme or through the phosphatidylethanolamine (PE) N-methyltransferase (PEMT) pathway. The PC/PE content ratio exhibited a daily variation with lowest levels at night, while *ChoK $\alpha$*  and *PEMT* mRNA expression displayed maximal levels at nocturnal phases. Our results demonstrate that mouse liver GPL metabolism oscillates rhythmically with a precise temporal control in the expression and/or activity of specific enzymes.

**Keywords:** Circadian rhythm, mouse liver, peripheral oscillator, phospholipid metabolism

## INTRODUCTION

The circadian timing system comprises central and peripheral oscillators distributed throughout the body to temporally regulate physiology and behavior with a period near 24 h. Circadian clocks are present in most living organisms, even in single cells, and regulate a number of physiological and biochemical rhythms (Dunlap et al., 2004). In mammals, the master circadian clock is located in the hypothalamic suprachiasmatic nuclei (SCN), while a number of peripheral oscillators have been described in different organs and tissues, such as the retina, liver, spleen, lung, pituitary gland, etc. (Mohawk et al., 2012). Moreover, circadian clocks present in immortalized cell lines and primary cell cultures display rhythms in gene expression and metabolic activities (Acosta-Rodríguez et al., 2013; Balsalobre et al., 1998; Marquez et al., 2004; Nagoshi et al., 2005). At the molecular level, the clock is controlled by a transcriptional/translational feedback circuitry

generating profiles of gene expression under a circadian base (Mohawk et al., 2012).

The murine liver constitutes a very intriguing model of a peripheral oscillator for investigating the circadian regulation of cellular metabolisms, hepatocyte cell regeneration and the impact of different diet compositions (Matsuo et al., 2003). Several transcriptomic, proteomic, lipidomic and metabolomic studies in mammalian tissues including the liver reveal a tight cross-talk between cell metabolism including that for lipids and the circadian clock (Adamovich et al., 2014; Asher & Schibler, 2011; Bass & Takahashi, 2010; Eckel-Mahan et al., 2012; Huang et al., 2011; Hughes et al., 2009; Menger et al., 2007; Reddy et al., 2006; Sahar & Sassone-Corsi, 2012), particularly where lipid metabolism is involved (Adamovich et al., 2014; Asher & Schibler, 2011; Bass & Takahashi, 2010; Bray & Young, 2011; Eckel-Mahan et al., 2012). Furthermore, the disruption of the molecular clock may cause a number of metabolic

Submitted May 24, 2014, Returned for revision July 14, 2014, Accepted July 26, 2014

Correspondence: Dr Mario E. Guido, Departamento de Química Biológica, Facultad de Ciencias Químicas, CIQUIBIC (CONICET), Universidad Nacional de Córdoba, Haya de la Torre s/n, Ciudad Universitaria, 5000 Córdoba, Argentina. Tel: 54-351-5353855; Ext.3429/30. Fax: 3406. E-mail: mguido@fcq.unc.edu.ar

disorders, such as the metabolic syndrome implicated in obesity, diabetes, hyperlipidemia, etc. (Durgan & Young, 2010; Froy, 2010; Green et al., 2008; Maury et al., 2010; Sookoian et al., 2008; Takahashi et al., 2008).

Glycerophospholipids (GPLs) are bioactive molecules of fundamental importance as structural components of all biological membranes and key cellular components involved in cell signaling, energy balance, vesicular transport, cell to cell and intracellular communication (Coleman & Mashek, 2011; Hermansson et al., 2011; Van Meer et al., 2008). GPLs are first synthesized from glycerol-3-phosphate via a *de novo* pathway formerly described by Kennedy and Weiss (Hermansson et al., 2011; Kennedy & Weiss, 1956) and subsequently remodeled by the Lands Cycle, involving the sequential activity of phospholipase A (PLA) and lysophospholipid acyl transferases (LPLATs) (Shindou & Shimizu, 2009; Shindou et al., 2009).

Phosphatidylcholine (PC) is an abundant and essential GPL present in the liver that plays an important role in the structural composition of hepatic membranes and in the generation of second messengers involved in key regulatory functions and other processes in this organ (Exton, 1994; Gehrig et al., 2008; Kent, 2005). PC synthesis is crucial for hepatocyte growth, liver cell proliferation and survival (Cui & Houweling, 2002). In mammals, the disruption of genes encoding phospholipid biosynthetic enzymes has severe physiological consequences or lethality (Vance & Vance, 2009). In the liver, the biosynthesis of PC may occur via the Kennedy pathway or through an alternative biosynthetic route in which the enzyme Phosphatidylethanolamine (PE) N-methyltransferase (PEMT) converts PE into PC (Li & Vance, 2008). The Kennedy pathway for PC synthesis involves three enzymatic steps catalyzed by choline kinase (ChoK), CTP: phosphocholine cytidyltransferase (CCT) and CDP-choline: 1,2-diacylglycerol cholinephosphotransferase (CPT) in which CCT and ChoK activities are considered the rate-limiting and regulatory steps under most metabolic conditions (Li & Vance, 2008). Nevertheless, it has been demonstrated that the availability of DAG also influences PC biosynthesis (Araki & Wurtman, 1998; Kent, 2005; Marcucci et al., 2010). Remarkably, in most mammals, there are two genes encoding for ChoK: *Chka* codes for ChoK $\alpha$ 1/2 and *Chkb* codes for ChoK $\beta$  (Aoyama et al., 2004; Wu & Vance, 2010). Mice lacking *ChoK $\alpha$*  die early in embryogenesis (Vance & Vance, 2009), while ChoK overexpression has been implicated in human carcinogenic processes (Gallego-Ortega et al., 2011; Glunde et al., 2011). In mice there are two genes for CCT: *Pcyt1a* encodes the CCT $\alpha$  protein from alternative transcripts termed CCT $\alpha$ 1 and CCT $\alpha$ 2 and the *Pcyt1b* gene encodes the CCT $\beta$ 2 and CCT $\beta$ 3 proteins from the differentially alternative spliced mRNAs CCT $\beta$ 2 and CCT $\beta$ 3 (Karim et al., 2003).

At present, little is known about the temporal regulation of GPL and PC biosynthesis by its intrinsic

circadian clock. In this connection, day/night changes in PC content and of other GPLs have been reported in the whole brain of rats maintained under a regular LD cycle (Díaz-Muñoz et al., 1987) but not under constant environmental conditions. However, no major conclusions can be drawn from this study since the brain displays an heterogeneous behavior in the different regions or nuclei examined, exhibiting different circadian phases or arrhythmicity (Abe et al., 2002). Similarly, another study showed significant variations in the phospholipid content of the liver in hamsters only under the LD cycle, and not under constant illumination conditions (Ginovker & Zhikhareva, 1982). It is noteworthy that continuous light is required to reveal whether temporal changes are generated in an endogenous and self-sustained manner as expected for circadian rhythms. In this connection, we have previously described that *de novo* synthesis of whole phospholipids in different cell types from mammalian and non-mammalian vertebrates is controlled by a circadian clock as observed in chicken retinal neurons *in vivo* or *in vitro* (Garbarino-Pico et al., 2004, 2005; Guido et al., 2001) as well as in quiescent murine fibroblasts after synchronization by a serum shock (Acosta-Rodríguez et al., 2013; Bray & Young, 2011; Marquez et al., 2004). Moreover, an extensive liver lipidomic analysis in wild-type and clock-disrupted mice kept in constant darkness (DD) and subjected to different feeding regimes, has shown that some triglycerides, GPLs and lipid regulators oscillated in their endogenous levels in both mouse strains (Adamovich et al., 2014).

Here, we studied whether GPL metabolism is temporally regulated in the mammalian liver under circadian clock control at the early stages of *de novo* biosynthesis and remodeling events. In addition, we have specially focused on the pathways of PC synthesis, investigating the expression and/or activity of its synthesizing enzymes. To this end, we performed circadian studies on liver samples collected at different phases/times from animals kept under a regular LD cycle or released to DD for 48 h. In our experimental design, mice were maintained with food and water *ad libitum* in order to address only the synchronizing effects of the light regardless of the food composition and accessibility. We first examined the temporal regulation of individual endogenous GPLs and of the activity of phosphatidate phosphohydrolase 1 (PAP-1/lipin) in desphosphorylating PA to DAG, a branching point for *de novo* synthesis of most GPLs (Csaki et al., 2013; Kok et al., 2012; Pascual & Carman, 2013). We then assayed LPLAT activities involved in the remodeling of membrane phospholipids. Finally, after evaluating possible changes over time in the endogenous content of PC and PE and in the PC to PE ratio, we examined the temporal control in the expression and/or activity of the two key synthesizing enzymes, ChoK and CCT from the Kennedy pathway as well as the expression of the key enzyme PEMT in the alternative liver route.

## EXPERIMENTAL PROCEDURES

### Materials

All reagents were of analytical grade. Alugram SIL G/UV<sub>254</sub> TLC silica gel 60-precoated sheets were from Macherey-Nagel (Duren, Germany). Phospholipid standards, MgCl<sub>2</sub> and ATP were from Sigma (St. Louis, MO). The Bio-Rad Protein Assay based on Bradford method was used to measure the protein concentration (Bradford, 1976).

TRIzol reagent (Invitrogen – Life Technologies, Carlsbad, CA, Cat.# 15596-026); for RT-PCR the reagents were from Promega (Madison, WI): DNAsa (RQ1 RNase-Free Dnase. Cat. #M6101), M-MLV (– Cat. #1701/1705 – Part #9PIM170), GoTaq DNA Polymerase (– Cat. #M3001/M3005/M3008), random primers and dNTPs.

SYBR Green PCR Master Mix (Applied Biosystems (Life Technologies, Carlsbad, CA) – Part #4309155). Protease inhibitors were from Sigma-Aldrich (Protease inhibitor cocktail, Cat. #P8340). Primers Taq-Man are shown in Supplementary Table 1; ATP-MgCl<sub>2</sub>, choline and p-choline were from Sigma-Aldrich, [<sup>14</sup>C]-choline from Perkin Elmer (Waltham, MA) (Product number: NEC141V, LOTE: 3614233, Specific Activity 55.19 mCi/mmol (0.2 mCi/ml; 55.19 mCi/mmol ≥0.1 uCi; 0.01812 mM in the reaction volume); the scintillation Cocktail was from Perkin Elmer – Optiphase HiSafe 3 (Cat. #1200- 437, 5L).

### Animal handling

Young male mice (*Mus musculus*) of the C57BL/6J strain were reared for at least 7 days on an LD cycle of 12 h each with food and water *ad lib* and a room temperature of ~20 °C. Then, animals were released to constant darkness (DD) for 48 h or kept under the same LD cycle. On day 10, animals were euthanized in the corresponding light condition at different times: 4, 8, 16 and 20 h during the regular LD cycle, or at 4, 8–9, 16, 20, 28, 32 and 40 h for those maintained in DD; for the dark condition a night viewer (IR viewer) was used. Livers were dissected out, immediately frozen in liquid air and then kept at –80 °C until homogenization. Since mice have free-running periods close to 24 h and they would not have shifted significantly after 48 h of DD, times of treatments were designated with respect to the previous entraining LD cycle (or zeitgeber) as ZTs for those animals kept under the LD cycle and as circadian times (CTs) for animals released to DD for 48 h. Thus, ZT 0 corresponds to the phase of the previous dark–light transition (subjective dawn), while ZT 12 corresponds to the time of the light–dark transition (subjective dusk) at which lights are turned off.

Animal handling was performed according to the *Guide to the Care and Use of Experimental Animals* published by the Canadian Council on Animal Care and approved by the local animal care committee (School of Chemistry, National University of Cordoba, Exp. 15-99-39796) and conforms to international ethical standards (Portaluppi et al., 2010).

### Preparation of liver homogenates

For PAP-1/lipin and LPLAT enzyme activities and phospholipid extraction, 200 µl of each liver dissected from mice euthanized at different times were homogenized in 1.5 ml of PBS containing protease inhibitors in a glass homogenizer by 20 strokes. Aliquots from total homogenates were used to quantify the protein content by the Bradford method (Bradford, 1976). Samples for PAP-1/lipin and LPLAT activities were lyophilized and stored at –80 °C until use. For mRNA extraction and RT-PCR (at end point and real time) the tissue was processed according to TRIzol reagent's manufacturer instructions.

For ChoK enzymatic activity, livers were homogenized in a glass homogenizer and then sonicated for 30 s. One volume of the homogenate was then resuspended in three volumes of the homogenization buffer (0.25 M sucrose = 8.56% M/V, protease inhibitor, 0.28% of B-mercaptoethanol). Samples were centrifuged for 5 min at 10 000 rpm, the pellet was discarded and protein content determined according to Bradford (1976). Supernatants were stored at 4 °C up to determination of the enzymatic activity according to Weinhold & Rethy (1974) and Weinhold et al. (1991).

### Phospholipid extraction, quantification and chromatographic separation

The extraction and quantification of endogenous phospholipids was determined according to Fine & Sprecher (1982) and Churchward et al. (2008a), with modifications. Total phospholipids were extracted with 20 volumes of chloroform/methanol (1:1, v/v) as described (one volume of homogenate contains ~100 µg of total protein). After 1 h at room temperature, extracts were centrifuged at 10 000 rpm × 30 min. Supernatants were resuspended in four volumes of distilled H<sub>2</sub>O until the separation into two phases was clearly visualized. These were then mixed by inversion four times and kept at 4 °C overnight. The aqueous phase was discarded and the organic phase was dried with N<sub>2</sub>. Finally, lipids were resuspended in 40 µl of chloroform–methanol (1:1)/volume of homogenate.

Individual phospholipids were separated in silica gel 60 plates soaked in 1.2% H<sub>3</sub>BO<sub>3</sub> (in ethanol:water 1:1) (from Macherey-Nagel, Duren, Germany) by a solvent system composed of chloroform:methanol:water:ammonium hydroxide (120:75:6:2 v/v) as described by Fine & Sprecher (1982). Standards and individual lipid species were visualized by using 3% cupric acetate in 8% phosphoric acid and then heated at 170 °C for 10 min in oven (modified from Churchward et al., 2008a).

### Image processing for the determination of individual phospholipid content

Two variables were calculated to estimate the signal intensity from the individual phospholipid bands. The first, termed “relative level”, represents the ratio between the signals of one individual phospholipid of

each sample and the averaged signal of this individual lipid in all samples; changes in this variable are an estimation of changes observed in individual phospholipid quantities. The second variable, “relative contribution”, is the ratio between the signal of one individual phospholipid and the sum of all phospholipids from the same sample. This is a close approximation to the proportion of each phospholipid in the total membrane. The PC/PE ratio was calculated as the ratio between the PC and PE content of each sample irrespective of any form of normalization.

#### ***In vitro* determination of LPLAT**

Liver homogenates were lyophilized and resuspended in ultrapure H<sub>2</sub>O containing protease inhibitors. Cell homogenates were used as a source of enzyme and endogenous lysophospholipids for determination of total LPLAT activity. The activity of liver LPLAT was determined as “*in vitro*” labeling by measuring the incorporation of [<sup>14</sup>C]-oleate from [<sup>14</sup>C]-oleoyl-CoA (56 mCi/mmol) into different endogenous lysophospholipid acceptors as described by Castagnet & Giusto (2002), Garbarino-Pico et al. (2004) and Acosta-Rodríguez et al. (2013). Under these experimental conditions, changes in the measured activity may reflect changes both in the amount of active enzyme and in the content of endogenous lysophospholipids. The incubation mixture for the assay contained 60 mM Tris-HCl (pH 7.8), 4 μM [1-<sup>14</sup>C]-oleoyl-CoA (10<sup>5</sup> dpm/assay), 10 mM MgCl<sub>2</sub>, 10 mM ATP, 75 μM CoA and 80 μg of homogenates in a final volume of 150 μl. The reaction was incubated for 10 min with shaking at 37 °C and stopped by addition of 5 ml chloroform/methanol (2:1, v/v). The lipids were extracted according to the method of Folch et al. (1957). The lipid extract was dried under N<sub>2</sub>, resuspended in chloroform/methanol (2:1, v/v) and spotted on silica gel H plates. Unlabeled phospholipids were used as standards. The chromatograms were developed by two-dimensional TLC using as system solvents chloroform/methanol/ammonia (65:25:5, v/v/v) in the first dimension and chloroform/acetone/methanol/acetic acid/water (30:40:10:10:4, v/v/v/v) in the second, followed by visualization with iodine vapors. The spots corresponding to PA, PC, PE, PI and PS were scraped off and radioactivity was determined by liquid scintillation.

#### **Determination of PAP-1/lipin activity**

Liver homogenates were resuspended in ultrapure H<sub>2</sub>O containing protease inhibitors. PAP-1/lipin activity was determined by monitoring the rate of release of 1,2 diacyl-[2-<sup>3</sup>H]-glycerol (DAG) from [2-<sup>3</sup>H]-phosphatidic acid (PA) as previously described by Pasquaré and Giusto (Acosta-Rodríguez et al., 2013; Garbarino-Pico et al., 2004; Pasquaré de García & Giusto, 1986; Pasquaré & Giusto, 1993). The reaction was stopped at 20 min by addition of chloroform/methanol (2:1, v/v). DAG was separated by TLC and developed with hexane:diethyl

ether:acetic acid (35:65:1, v/v/v) (Giusto & Bazan, 1979). To separate monoacylglycerol (MAG) from PA, the chromatogram was developed with hexane/diethyl ether/acetic acid (20:80:2.3, v/v/v) as developing solvent. PAP activity was expressed as the sum of labeled DAG plus MAG (h × mg of protein)<sup>-1</sup>.

#### ***In vitro* assessment of ChoK enzyme activity**

Liver homogenates were prepared as indicated above. 100 μg of protein homogenate were assessed with 0.5 μl [methyl-<sup>14</sup>C]-choline chloride (55.19 mCi/mmol specific activity), 10 mM ATP, 10 mM Mg<sup>2+</sup>, 0.1 M Tris-HCl (pH 8) and water to a final volume of 100 μl, according to Weinhold et al. (1991) and Acosta-Rodríguez et al. (2013). The reaction was stopped at 10 min by an addition of 1 ml of chloroform on ice. The soluble products were extracted using chloroform/methanol (2:1, v/v) and separated by TLC. The solvent system was 0.9% NaCl/methanol/NH<sub>4</sub>OH (50:70:5, v/v/v). The TLC-separated product was autoradiographed and the bands corresponding to [<sup>14</sup>C]-choline and [<sup>14</sup>C]-phosphocholine were scraped and quantified adding 1 ml of scintillation cocktail in a liquid scintillation counter. The time reaction (10 min at 37 °C) and protein concentration (100 μg) were selected from a linear range of time- and enzyme-curves.

#### **RNA isolation and reverse transcription**

Total RNA was extracted from liver homogenates using TRIzol<sup>®</sup> reagent following manufacturer's specifications (Invitrogen). The yield and purity of RNA were estimated by optical density at 260/280 nm. 1 μg of total RNA was treated with DNase (Promega, Madison, WI) and utilized as a template for the cDNA synthesis reaction using ImPromII reverse transcriptase (Promega, Madison, WI) and an equimolar mix of random hexamers and oligo-dT (Biodynamics, Buenos Aires, Argentina) in a final volume of 25 μl according to manufacturer's indications.

#### **PCR assay (endpoint PCR)**

The primers used for RT-PCR are listed in Supplementary Table 1. The polymerase chain reaction was performed in a Labnet Multigen Thermal cycler using the GoTaq<sup>®</sup> DNA Polymerase (Promega). PCR reactions were carried out with an initial denaturation step of 4 min at 94 °C, 35 cycles of 60 s at 94 °C, 30 s at 60 °C and 30 s at 72 °C, and a final 5-min elongation step at 72 °C. Amplification products were separated by 1% agarose gel electrophoresis and visualized by ethidium bromide staining.

#### **Real-time PCR (qPCR)**

Quantitative RT-PCR was performed using SYBR Green or TaqMan Gene Expression Assays in a Rotor Q Gene (Qiagen, Valencia, CA). The primer/probe sequences are summarized in Supplementary Table 1. The

amplification mix contained 1  $\mu$ l of the cDNA, 1  $\mu$ l 20 $\times$  mix primer/probe or 250 nM Forward–Reverse TBP primers, and 10  $\mu$ l of Master Mix 2 $\times$  (Applied Biosystem) in a total volume of 20  $\mu$ l. The cycling conditions were 10 min at 95.0  $^{\circ}$ C, and 45 cycles of 95.0  $^{\circ}$ C for 15 s, 60.0  $^{\circ}$ C for 30 s and 72  $^{\circ}$ C for 30 s. The standard curve linearity and PCR efficiency (E) were optimized. We used the  $2^{-\Delta\Delta C_T}$  according to Livak & Schmittgen (2001), and Larionov et al. (2005) and TBP as the reference gene (Acosta-Rodríguez et al., 2013).

We used the equation described by Livak & Schmittgen (2001)

$$x = \frac{x_0}{r_0} = \frac{x_{xT} \cdot (1 + E_x)^{-\Delta C_{xT}}}{r_{rT} \cdot (1 + E_r)^{-\Delta C_{rT}}}$$

in which  $x$  is the relative level of the mRNA of interest (problem),  $x_0$  and  $r_0$  are the initial amounts for the problem and reference mRNAs, respectively;  $x_{xT}$  and  $r_{rT}$  are the amounts for the problem and reference mRNAs, respectively, when the signal reaches the threshold of detection established for each case;  $E_x$  and  $E_r$  are the efficiencies in the amplification estimated for both mRNAs (problem and reference), respectively;  $\Delta C_{xT}$  and  $\Delta C_{rT}$  are the differences in the number of amplification cycles needed to reach the threshold of expression for both transcripts (problem and reference), respectively, from the problem sample tested as compared with a sample having a concentration equal to 1, previously established according to the regression of the calibration curve.

Each RT-PCR quantification experiment was performed at least in duplicate (TaqMan or SYBR) for each sample ( $n = 2\text{--}5/\text{sample}$ ).

## Statistics

For LD data, statistical analyses involved a one-way analysis of variance (ANOVA) to test the time effect and Kruskal–Wallis (K–W) when the normality of residuals was infringed. Pairwise comparisons were performed by the Mann–Whitney (M–W) test when appropriate. For further periodic analysis of DD data, we performed a COSINOR analysis, and when the model assumptions were infringed we used a linear–circular correlation as described by Mardia (1976), with the Spearman coefficient followed by an aleatorization test with 1000 iterations to determine the  $p$  value. The analysis considered a period ( $\tau$ ) of 16, 20 and 24 h and significance at  $p < 0.05$ .

## RESULTS

### Determination of the mouse liver as a circadian oscillator

In order to investigate the temporal regulation of GPL metabolism in the liver of mice after LD synchronization, we first characterized the oscillatory capability of this organ in animals previously entrained to a regular LD cycle (for 7 days) and then released to DD or maintained in the same LD cycle for another 48 h. Livers collected at different times (ZTs or CTs) after synchronization displayed a significant circadian rhythmicity in mRNA levels of the clock gene *Bmal1* in either LD or DD conditions with a period ( $\tau$ )  $\sim 24$  h (Figure 1, Table 1); these observations are in agreement with previous reports (Hughes et al., 2009; Kornmann et al., 2007; Panda et al., 2002). The statistical analysis revealed a

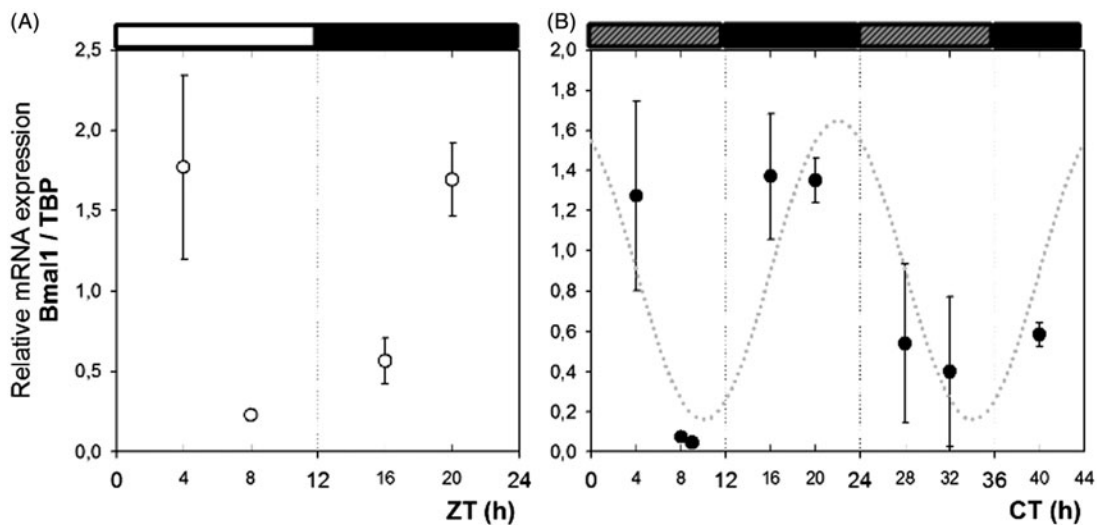


FIGURE 1. Expression of *Bmal1* mRNA in livers of mice synchronized to a 12:12h LD cycle for 7 days and released to constant darkness (DD) (right panel) or maintained in the LD cycle (left panel). Levels of *Bmal1* mRNA were assessed by RT-qPCR with RNA extracted from livers of animals collected at different times (ZTs for the LD cycle or CTs for DD) and normalized according to the expression of the housekeeping gene TBP. The ANOVA revealed a significant time effect on the levels of *Bmal1* transcripts (LD:  $p < 0.001$  and DD:  $p < 0.028$ ). The results are mean  $\pm$  SEM (triplicate samples from three independent experiments). The solid bars above the graphs (left panel) denote whether lights were on (white bar) or off (black bars) during the LD cycle; the hatched and solid bars above the graph (right panel) denote when lights were on (gray bar) or off (black bar), respectively, in previous days.

TABLE 1. Statistical analysis was performed with results from 5 independent samples for each ZT in LD and 2–3 independent samples for each CT in the DD condition. One-way ANOVA (or Kruskal–Wallis when appropriate) was used to test the time effect in the LD condition and COSINOR or linear-circular correlation with the Spearman coefficient followed by an aleatorization was applied to test periodicity in DD. Acrophase denotes the time at which the variable reaches the maximum value.

	LD		DD			
	ANOVA		COSINOR		Acrophase (CT)	Period ( $\tau$ , h)
	$R^2$ -aj ( $n$ )	$p$ Value	$R^2$ -aj ( $n$ )	$p$ Value		
<b>A – Phospholipids</b>						
PC/PE	0.057 (20)	ns <sup>a</sup>	0.443 (20)	0.0008 <sup>c</sup>	4	24
PC levels	0 (20)	ns <sup>a</sup>	0.158 (20)	0.047 <sup>c</sup>	8	24
PE levels	0.113 (20)	ns <sup>a</sup>	0.188 (20)	ns <sup>d</sup>		24
PI levels	0.097 (20)	ns <sup>a</sup>	0.188 (20)	0.032 <sup>c</sup>	9	24
SM+PS levels	0.263 (20)	0.049 <sup>a</sup>	0.215 (20)	ns <sup>d</sup>		24
PC contribution	0 (20)	ns <sup>a</sup>	0.083 (20)	ns <sup>c</sup>		24
PE contribution	0.147 (20)	ns <sup>a</sup>	0.238 (20)	ns <sup>d</sup>		24
PI contribution	0.289 (20)	0.037 <sup>a</sup>	0.011 (20)	ns <sup>d</sup>		24
SM+PS contribution	0 (20)	ns <sup>a</sup>	0.203 (20)	0.026 <sup>c</sup>	9	24
<b>B – mRNA Expression</b>						
Bmal1	0,446 (20)	0.0012 <sup>b</sup>	0,344 (20)	0.029 <sup>d</sup>	22	24
Chok $\alpha$	0,566 (20)	0.0009 <sup>a</sup>	0,333 (20)	0.045 <sup>d</sup>	22	24
Chok $\beta$	0 (20)	ns <sup>a</sup>	0,177 (20)	0.037 <sup>c</sup>	8	16
pemt	nd		0,315 (20)	0.0059 <sup>c</sup>	19	24
Cct $\alpha$ 1	0 (20)	ns <sup>a</sup>	nd			
<b>C – Enzymatic activity</b>						
ChoK	0 (20)	ns <sup>a</sup>	0.040 (20)	ns <sup>c</sup>		16
MAGL	0.426 (8)	ns <sup>a</sup>	0.285 (16)	0.125 <sup>d</sup>		24
PAP1	0.485 (8)	ns <sup>a</sup>	0.270 (16)	0.023 <sup>c</sup>	11	24
LPAAT	0.831 (8)	0.017 <sup>a</sup>	0.712 (16)	0.000024 <sup>c</sup>	12	24
LPCAT	0.481 (8)	ns <sup>a</sup>	0.616 (16)	0.00019 <sup>c</sup>	15	16
LPEAT	0.207 (8)	ns <sup>a</sup>	0.317 (16)	0.013 <sup>c</sup>	14	24
LPIAT	0.048 (8)	ns <sup>b</sup>	0.461 (16)	0.0023 <sup>c</sup>	13	16
LPSAT	0.690 (8)	0.055 <sup>a</sup>	0.185 (16)	0.055 <sup>c</sup>		16

<sup>a</sup>ANOVA; <sup>b</sup>Kruskal–Wallis; <sup>c</sup>COSINOR;

<sup>d</sup>Linear–circular correlation.

NS: non-significant ( $p > 0.05$ ).

significant effect of time in both conditions ( $p < 0.0012$  for the LD cycle and  $p < 0.029$  for DD, see Table 1).

### Circadian changes in the endogenous levels of GPLs

To determine whether the metabolism of phospholipids varies throughout the day we first examined the content of endogenous GPLs across time in both LD and DD conditions. The results showed a significant daily variation in relative levels obtained in DD (PC:  $p < 0.047$ , PI:  $p < 0.032$ , PE: N.S.) (Figure 2, Table 1). Remarkably, in DD the endogenous content (relative levels) of diverse GPLs exhibited a 2- or 3-fold change over time with the highest levels during the subjective day along two cycles examined of 24 h each (CTs 8 and 32) and lowest levels at CTs 20 and 40 during the subjective night. Moreover, although levels of PE did not vary significantly over time, the PC to PE ratio displayed a marked oscillation in DD ( $p < 0.0008$  by COSINOR) with higher ratios during the day and lower ratios at night (Figure 3). By contrast, slight changes were found in the relative contribution of individual phospholipids (Supplementary Figure 1), each one showing an idiosyncratic pattern and only SM+PS presenting a circadian profile. In LD, we found significant effects of time only in relative levels of

SM+PS and in the relative contribution of PI (Table 1; Figure 2E–G, left panel and Supplementary Figure 1); no similar temporal profiles were seen in GPL content for LD and DD conditions, likely reflecting a differential effect of the light exposure during the L-phase. However, similar patterns of oscillation were observed in the PC/PE ratio in both illumination conditions, with higher levels during the L-phase or subjective day. Overall, observations in DD are in agreement with a recent report based on lipidomic analysis showing daily oscillations in the endogenous content of triglycerides and some GPLs in the liver of mice maintained in DD and either fed *ad libitum* or night fed (Adamovich et al., 2014).

### Daily variation in the activity of different mouse liver phospholipid synthesizing enzymes

Although the steady state of endogenous GPLs could be the combined outcome of the biosynthesis and the degradation processes at any time, we explored here the possibility that the circadian changes observed in the endogenous content of GPLs in livers from mice kept in DD after synchronization, were due to variations in the activity of enzymes involved in the *de novo*

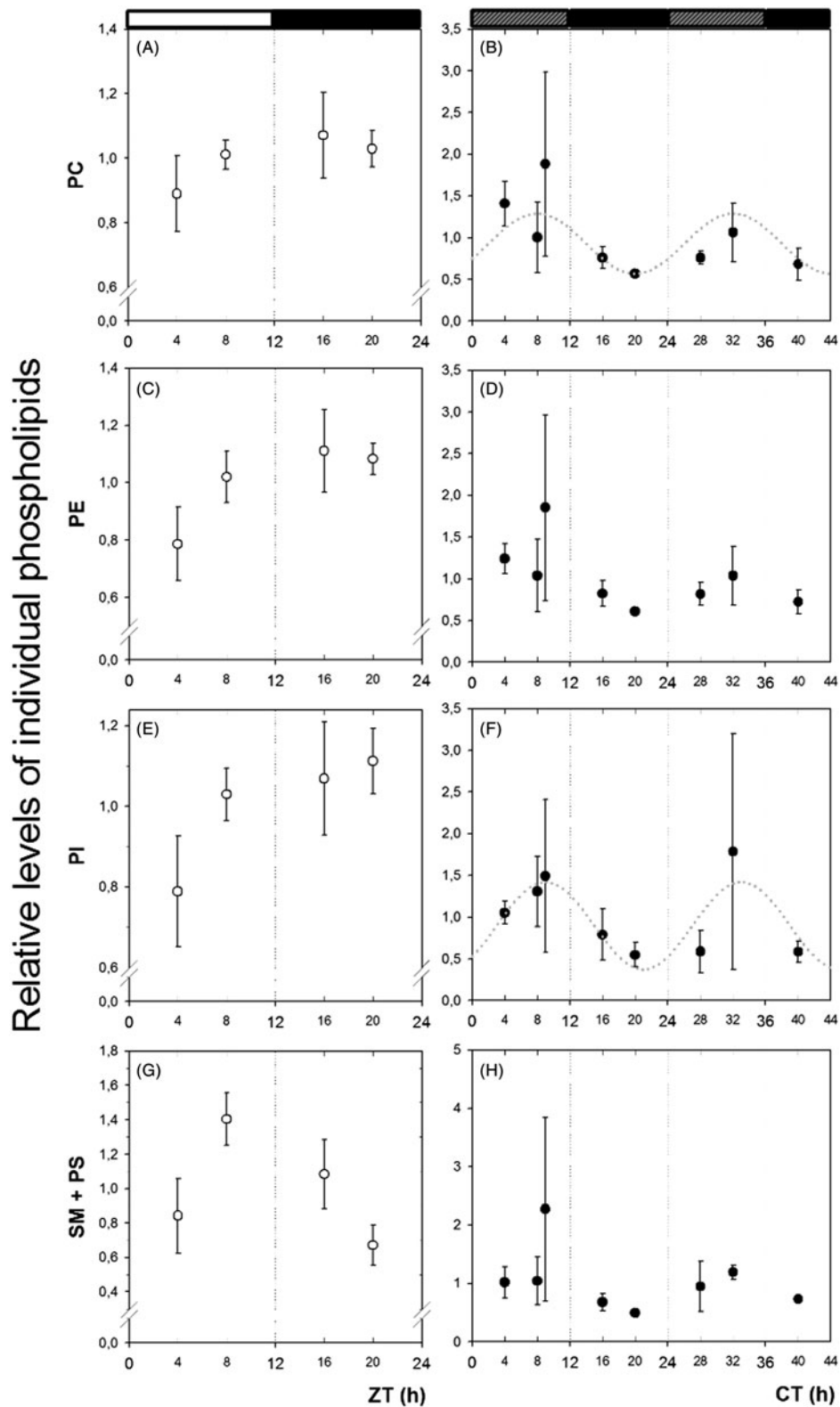


FIGURE 2. Daily variation in the endogenous levels of different glycerophospholipids extracted from livers of mice synchronized to a 12:12 h LD cycle for 7 days and released to constant darkness (DD) (right panels) or maintained in the LD cycle (left panels). Samples were collected at different times (ZTs for the LD cycle or CTs for DD) and processed as described in Experimental Procedures. Results are the mean  $\pm$  SEM (in LD:  $n=5$ /group; in DD:  $n=2-3$ /group). The COSINOR revealed a significant effect of time for PC and PI in DD ( $p \leq 0.05$ ). See text for further details and Table 1 for the statistical analysis. The solid bars above the graphs (left panel) denote whether lights were on (white bar) or off (black bars) during the LD cycle; the hatched and solid bars above the graph (right panel) denote when lights were on (gray bar) or off (black bar), respectively, in previous days. PC: Phosphatidylcholine, PE: Phosphatidylethanolamine, PI: Phosphatidylinositol and PS+SM: Phosphatidylserine plus Sphingomyelin.

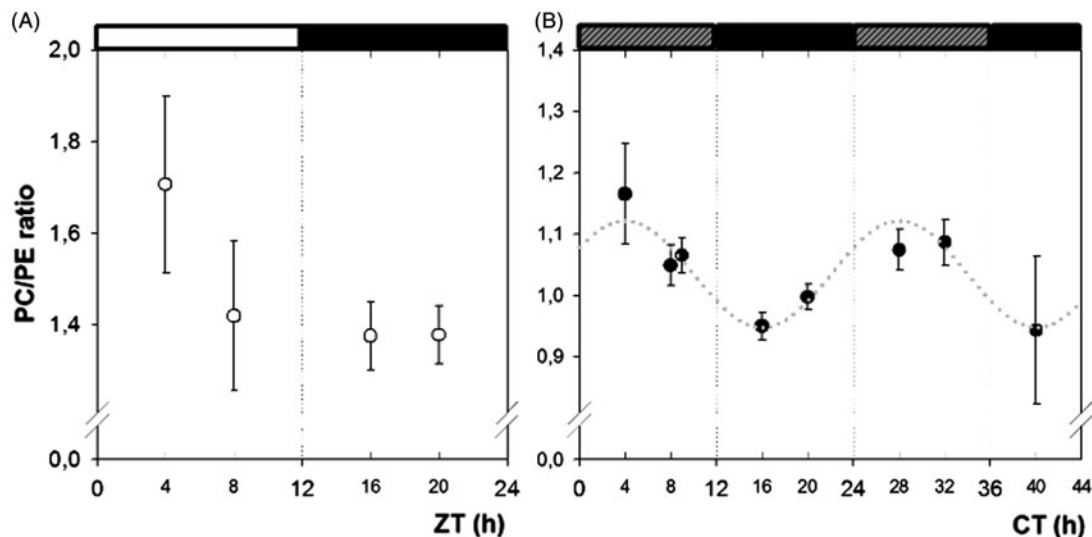


FIGURE 3. Ratio of PC to PE content from liver samples of mice synchronized to a 12:12 h LD cycle for 7 days and released to constant darkness (DD) (right panel) or maintained in the LD cycle (left panel). Samples were collected at different times (ZTs for the LD cycle or CTs for DD) and processed as described in Experimental Procedures. Results are the mean  $\pm$  SEM (in LD:  $n = 5$ /group; in DD:  $n = 2-3$ /group). The COSINOR revealed a significant effect of time in the PC/PE ratio in both DD ( $p \leq 0.0008$ ). See text for further details and Table 1 for the statistical analysis. The solid bars above the graphs (left panel) denote whether lights were on (white bar) or off (black bars) during the LD cycle; the hatched and solid bars above the graph (right panel) denote when lights were on (gray bar) or off (black bar), respectively, in previous days.

synthesis of phospholipids. For this, we determined the *in vitro* activities of LPAAT and PAP-1/lipin in homogenates of mouse livers collected at different times (ZTs or CTs) in LD or DD, respectively (Figure 4).

#### **De novo synthesis: lysophosphatidic acid acyltransferase (LPAAT) activity**

PA, the main precursor of GPLs, is synthesized by the acylation of lysophosphatidic acid (LPA) catalyzed by LPAAT. In synchronized livers, the acylation of LPA exhibited a significant temporal variation in LD with the highest levels at ZTs 4 and 20 (Figure 4). Moreover, in DD the highest levels of PA production were seen during the day/night transition (dusk) at CTs 8–9 and 16, and at CTs 32 and 40 during the first and second cycles, respectively. The lowest levels of PA production by acylation were found at 8–16 h in LD and at CT 20 in DD (Figure 4, Table 1). The statistical analysis revealed a major effect of time on LPAAT activity in both LD and DD ( $p < 0.0017$  and  $p < 0.000024$  by COSINOR) with a clear 8 h-shift between the two conditions, likely indicating the differential effect of light exposure during the LD cycle.

#### **De novo synthesis: phosphatidate phosphohydrolase 1 (PAP-1)/lipin activity**

As precursor of all GPLs, PA is dephosphorylated to DAG by PAPs to synthesize PC and PE (Coleman & Mashek, 2011; Hermansson et al., 2011). Although there are two types of PAP activity – PAP-1/lipin and PAP-2/LPPs (Csaki et al., 2013; Kok et al., 2012; Pascual & Carman, 2013) – only PAP-1/lipin activity showed appreciable levels in mouse liver homogenates. Based on this

observation and since PAP-1/lipin is primarily involved in lipid synthesis in the endoplasmic reticulum, we focused our studies on PAP-1/lipin activity (see section “Methods” for further details). In synchronized mice kept in DD for 48 h, PAP-1 activity of liver homogenates exhibited a significant temporal variation with a period of 24 h, with the highest levels of DAG production at 8–9 and 40 h and the lowest levels at CT 20 (Figure 4). The statistical analysis by COSINOR showed time to have a major effect ( $p < 0.023$ ) and revealed that the maximum activity is at CT 11 with minimum levels around CT 23. No significant differences were found in LD; however, the temporal profiles of enzyme activity were similar in both illumination conditions with higher levels during the L phase of LD cycle or the subjective day.

#### **Temporal contribution of lysophospholipid acyltransferase (LPLAT) activities to GPL remodeling in the mouse liver**

To evaluate whether the remodeling of GPLs varies over time, we assessed the activity of LPLATs involved in the acylation of lysophospholipids (Lands cycle) in the mouse liver of animals kept in LD or DD after 7-days synchronization. We found no significant time differences in the LD situation for most LPLATs assessed (Figure 5, left panel). By contrast, a remarkable temporal variation in the activity of LPLAT for the different GPLs examined was found in homogenates obtained at different times in DD (Figure 5, right panel; Table 1 – Part C). The statistical analysis revealed a major effect of time for LPLAT activity irrespective of the lysophospholipid assessed ( $p \leq 0.05$  by COSINOR); in addition, a rhythmic pattern was observed for the different GPLs



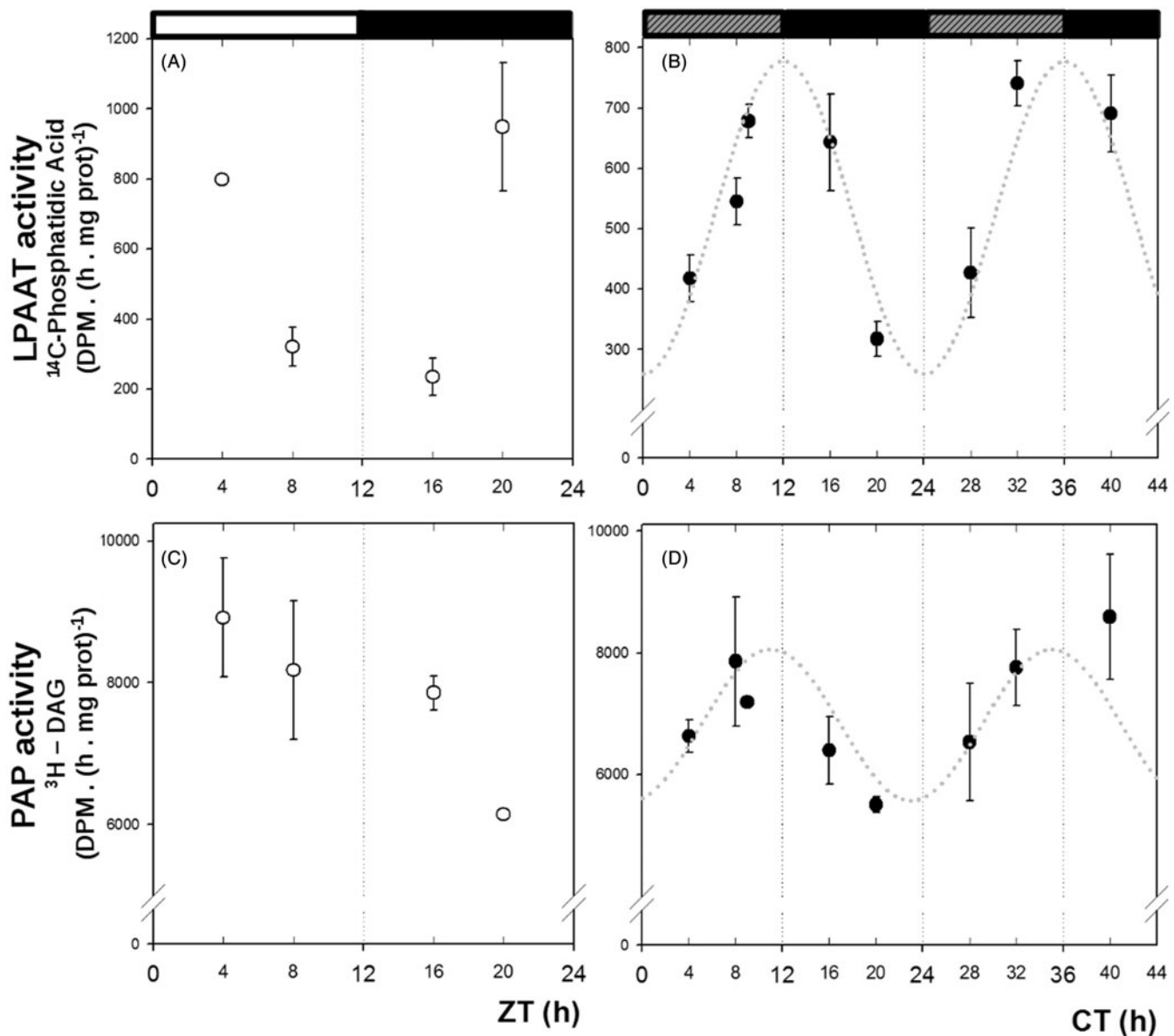


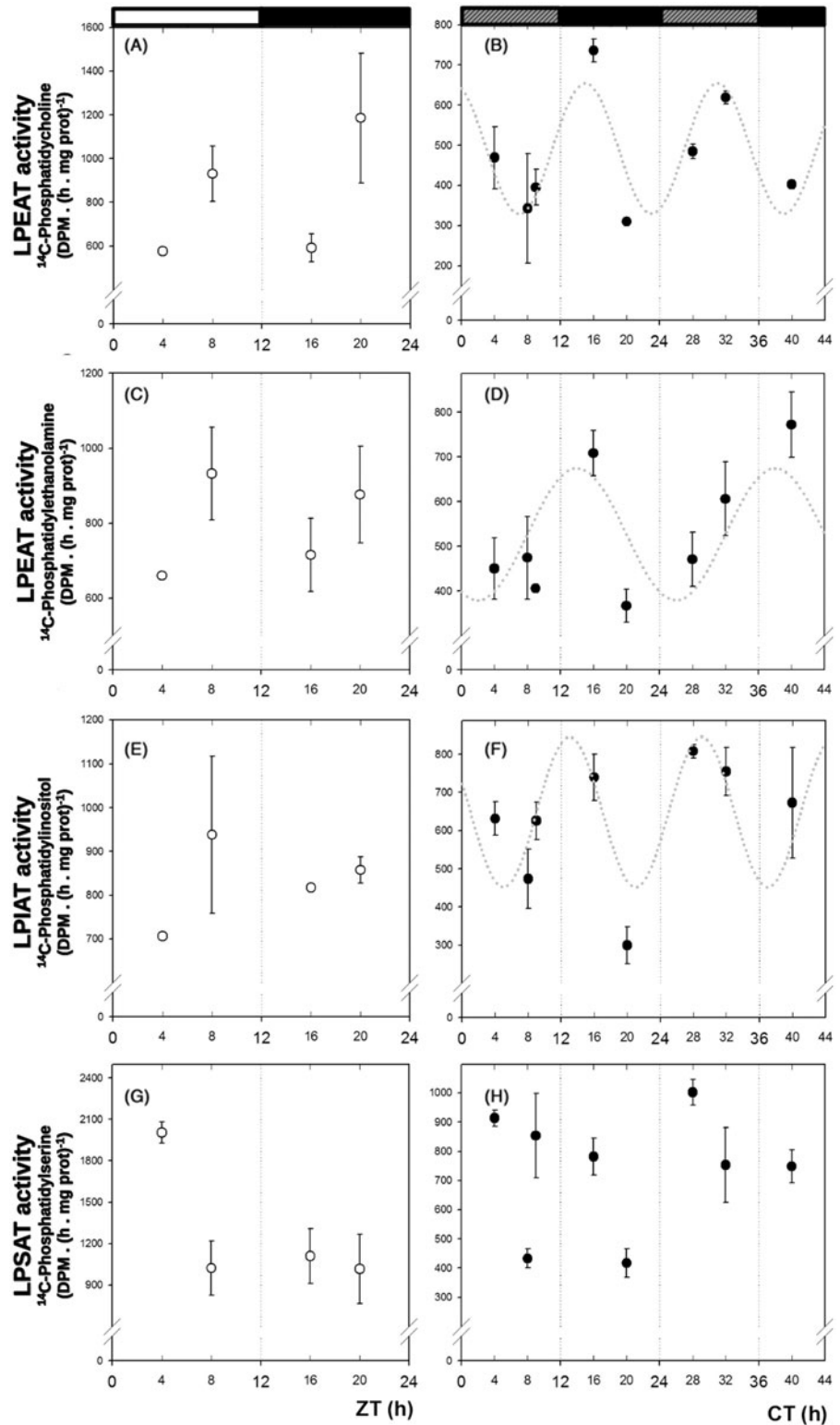
FIGURE 4. Daily variation in the activities of lysophosphatidic acid acyltransferase (LPAAT) and of phosphatidate phosphohydrolase 1 (PAP-1/lipin) in mouse liver from animals synchronized to a 12:12h LD cycle for 7 days and released to constant darkness (DD) (right panels) or maintained in the LD cycle (left panel). LPAAT activity was determined in homogenates of livers collected at different times (ZTs in LD or CTs in DD). The activity was measured by the incorporation of [<sup>14</sup>C]-oleate into lysophosphatidic acid (LPA). LPAAT activity exhibited significant temporal changes ( $p < 0.02$  in LD and  $p < 0.000024$  in DD). See text for further details and Table 1 for the statistical analysis. PAP-1/lipin activity was determined in mouse livers collected at different times (ZTs or CTs) as described in Experimental Procedures. The COSINOR analysis reveals a significant effect of time on enzyme activity ( $p = 0.023$ ) in DD. Results are the mean  $\pm$  SEM of 3 independent synchronization experiments ( $n = 2/\text{group}$ ). The solid bars above the graphs (left panel) denote whether lights were on (white bar) or off (black bars) during the LD cycle; the hatched and solid bars above the graph (right panel) denote when lights were on (gray bar) or off (black bar) respectively in previous days.

formed with a period ranging between 16 and 24 h. Remarkably, for most LPLAT activities, the highest levels were seen at CT 16 and the lowest at CT 20. Moreover, we found a significant 100–160% variation in activities over time between maximum and minimum values (Figure 5). In addition, it can be observed that the activity peak found at CT 20 for all LPLATs measured is markedly delayed with respect to the rhythm observed in the endogenous content (relative levels) of GPLs and PAP-1/lipin activity (Figures 2 and 4).

#### Circadian changes in PC content in the mouse liver

Since the endogenous levels of PC – the most abundant GPL in eukaryotic cells – displayed a significant temporal variation in the mouse liver of LD-entrained animals released to DD (Figure 2) as well as in its relative contribution as indexed by the PC/PE ratio, displaying highest levels at subjective midday (Figure 3), we further investigated the contribution of its different synthesizing enzymes. For this, we first assessed the expression at the mRNA level by RT-qPCR of the

FIGURE 5. Daily variations in lysophospholipid acyl transferase (LPLATs) activities in mouse liver from animals synchronized to a 12:12 h LD cycle for 7 days and released to constant darkness (DD) (right panel) or maintained in the LD cycle (left panel). LPLAT activity was determined in homogenates of livers collected at different times (ZTs in LD or CTs in DD). The activity was measured by the incorporation of [ $^{14}$ C]-oleate into lysophosphatidylcholine (LPC), lysophosphatidylethanolamine (LPE), lysophosphatidylinositol (LPI) and lysophosphatidylserine (LPS). The LPLAT activity exhibited significant temporal changes for all LPLs examined ( $p \leq 0.055$  by COSINOR). Results are the mean  $\pm$  SEM of 3 independent experiments ( $n = 2/$  group). The solid bars above the graphs (left panel) denote whether lights were on (white bar) or off (black bars) during the LD cycle; the hatched and solid bars above the graph (right panel) denote when lights were on (gray bar) or off (black bar), respectively, in previous days. See text for further details and Table 1 for the statistical analysis.



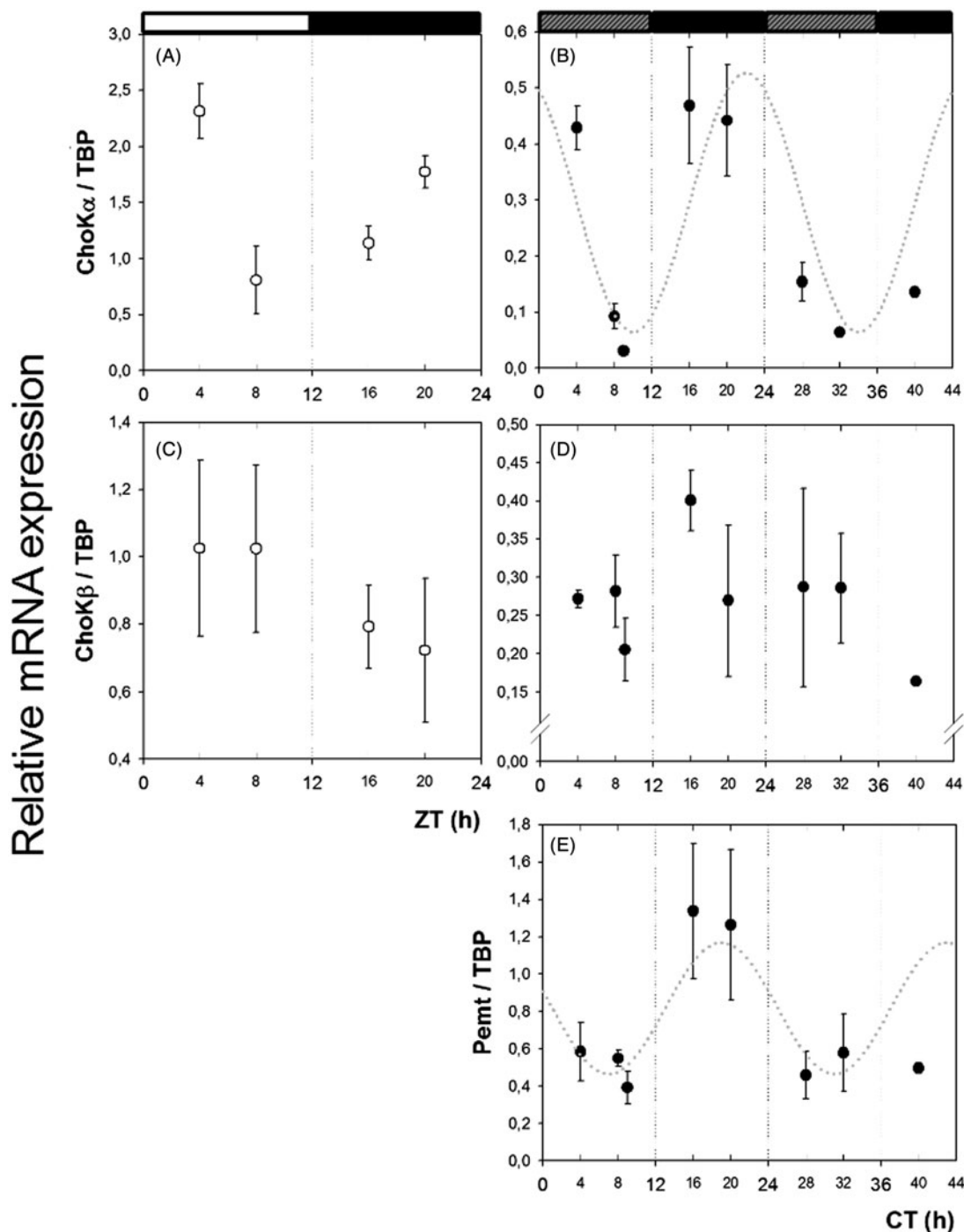


FIGURE 6. Temporal variation in the mRNA expression of *ChoK $\alpha$*  and  $\beta$  (A–D), and *PEMT* (E) in liver samples from animals synchronized to a 12:12 h LD cycle for 7 days and released to constant darkness (DD) (right panel) or maintained in the LD cycle (left panel). RT-qPCR was performed on RNA extracted from homogenates of livers collected at different times (ZTs for the LD cycle or CTs for DD) and normalized according to the expression of the housekeeping gene TBP. The ANOVA and linear-circular correlation revealed a significant time effect on levels of *ChoK $\alpha$*  in both LD and DD ( $p < 0.0009$  and  $p < 0.045$ , respectively) and of *PEMT* transcripts in DD ( $p < 0.006$ ). On the contrary, *ChoK $\beta$*  transcripts presented no significant variations at any time examined. The results are mean  $\pm$  SEM (triplicate from five independent samples for LD and triplicate from 2 to 3 independent samples for DD). The solid bars above the graphs (left panel) denote whether lights were on (white bar) or off (black bars) during the LD cycle; the hatched and solid bars above the graph (right panel) denote when lights were on (gray bar) or off (black bar), respectively, in previous days.

regulatory enzymes ChoK and CCT and the PEMT, which also appears to play an important role in the control of PC levels in the liver (Li & Vance, 2008). To this end, we studied the temporal profile of *ChoK $\alpha$*  and

*ChoK $\beta$*  transcripts in homogenate samples collected at different times in LD or DD conditions (Figure 6, Table 1 – Part B). The ANOVA revealed a significant time effect for *ChoK $\alpha$*  mRNA ( $p < 0.009$ ) in LD but not for *ChoK $\beta$*

transcript levels tested in the same illumination condition. Moreover, the periodic analysis shown in Table 1 – Part B indicates that levels of *ChoK $\alpha$*  mRNA robustly oscillate in DD with a period ( $\tau$ )  $\sim 24$  h ( $p \leq 0.045$ ) with the highest transcript levels during the subjective night (CTs 16–20), whereas *ChoK $\beta$*  also displayed a certain daily rhythmicity with a  $\tau \sim 16$  h ( $p < 0.04$ ) (Figure 6). Overall, similar temporal profiles in *ChoK $\alpha$*  mRNA levels were observed in both illumination conditions (LD and DD) with higher levels at early day and at mid-subjective night.

Nevertheless, we were unable to detect levels of ChoK proteins by WB in the homogenates, likely due to its low expression in non-tumor derived cells (Gallego-Ortega et al., 2011; Ramírez de Molina et al., 2002). Furthermore, no significant fluctuations were found in levels of total ChoK activity assessed, though a trend towards higher nocturnal levels was observed during subjective night (data not shown). As regards CCT expression, we detected appreciable levels of CCT $\alpha$ 1 by RT-PCR but not of CCT $\alpha$ 2 or CCT $\beta$ . Moreover, no significant time-related variations were seen in mRNA levels of CCT $\alpha$ 1 under the regular LD cycle ( $p = 0.694$  by ANOVA).

An alternative PC biosynthetic pathway taking place mainly in the liver involves PEMT activity that converts PE into PC (Li & Vance, 2008). We therefore evaluated PEMT mRNA expression by RT-qPCR. We found that levels of PEMT mRNA displayed a robust rhythmicity in DD with a period ( $\tau$ )  $\sim 24$  h ( $p \leq 0.006$  by COSINOR) with the highest levels during the subjective night (CTs 16–20).

## DISCUSSION

In the present work, we report for the first time that GPL metabolism in the mouse liver is subjected to temporal control in animals synchronized to a regular 12:12 h LD cycle for 7 days and then released to DD with food and water *ad lib*. In fact, the temporal variations observed in the content of endogenous GPLs and in the PC/PE ratio, as well as in the activity and expression of key biosynthetic lipidic enzymes, represent truly circadian metabolic rhythms with a period ( $\tau$ )  $\sim 24$  h along two cycles assessed in constant illumination conditions (DD). Interestingly, some of the parameters measured also presented a significant oscillation along the 24 h of the regular LD cycle condition (this work) or when mice from different strains (wt or clock-disrupted) were subjected to *ad libitum* or night feeding (Adamovich et al., 2014). Thus, both circadian clocks and feeding–fasting cycles play a major role in the regulation of triacylglycerol (TAG) and other lipid (PC, PE, PI) accumulation and whole endogenous levels in the liver; some oscillations of TAG and GPLs still persist even in the absence of a functional clock (*Per1/2*<sup>-/-</sup>), albeit with a completely different phase.

In order to validate our study model, we first of all looked for the expression of the clock gene *Bmall* at the mRNA level. We found a significant oscillation for this transcript in both illumination conditions (LD and DD), clearly showing that the mouse liver constitutes a useful model of a peripheral oscillator in mammals. Recent studies have clearly linked the molecular clock with the regulation of lipid metabolism, and the disruption of circadian clocks' results in pathophysiological changes resembling the metabolic syndrome in which lipid metabolism is strongly altered (Asher & Schibler, 2011; Bass & Takahashi, 2010; Bray & Young, 2011; Maury et al., 2010; Turek et al., 2005). We have previously shown that fibroblasts in culture exhibit circadian rhythms in the biosynthesis of radiolabeled phospholipids in clear antiphase with the rhythm in the clock gene *Per1* expression (Balsalobre et al., 1998; Marquez et al., 2004). Moreover, after knocking down *Per1* expression, the metabolic rhythm disappeared and cultures of *CLOCK* mutant fibroblasts – cells with an impaired clock mechanism – displayed a loss of rhythmicity in both *PER1* expression and phospholipid labeling; these results clearly indicate a tight control over phospholipid synthesis by the molecular circadian clock.

In this paper, we characterized the oscillatory behavior of *de novo* GPL biosynthesis and remodeling in the mouse liver from animals synchronized to environmental LD cycles and then kept in DD. Endogenous content (relative levels) of individual GPLs (PC, PI) showed a significant daily variation, with maximum levels during the subjective day and minimum values at subjective night. Moreover, despite the similarity of the PC and PE patterns, the ratio of PC to PE showed a marked variation over time following the same profile observed for individual GPLs, with minimum values found at midnight. It is known that membrane properties, such as fluidity are mainly regulated by the fatty acid composition of lipids; however, the temporal PC/PE variation observed may also contribute to substantial changes in the membrane properties (integrity, fluidity, curvature, etc.) (Churchward et al., 2008b; Li et al., 2006; Sen & Hui, 1988) and enzyme activity (Sleight & Kent, 1983) along the 24 h, possibly reflecting differential needs in membrane activity and functioning over time. In this connection, day/night changes observed in the endogenous content of individual GPLs may result from similar oscillations in the activity of the two key biosynthetic enzymes, LPAAT and PAP-1/lipin. It is noteworthy that enzymes involved in GPL metabolism have been shown to be highly regulated (Castagnet & Giusto, 2002; de Arriba Zerpa et al., 1999; Garbarino-Pico et al., 2004, 2005; Giusto et al., 2002, 2010). PAP-1/lipin, an enzyme that plays an essential role in phospholipid metabolism, dephosphorylates PA to DAG (Donkor et al., 2007; Reue & Brindley, 2008) whereas PAP-2/LPP (or lipid phosphate phosphatase) has been mainly implicated in signal transduction

mechanisms (Brindley, 2004; Giusto et al., 2000; Pasquare et al., 2004). Physiological functions affected by PAP activities include phospholipid synthesis, gene expression, nuclear/endoplasmic reticulum membrane growth, lipid droplet formation and vacuole homeostasis and fusion (reviewed in Pascual & Carman (2013); Kok et al. (2012)). In addition, lipin may play an important role in the regulation of lipid intermediates (PA and DAG) which influences essential cellular processes including adipocyte and nerve cell differentiation, adipocyte lipolysis and hepatic insulin signaling (reviewed in Csaki et al. (2013)). Remarkably, PC, PE and triacylglycerol are synthesized from DAG generated by PAP-1/lipin, whereas PA is the precursor for PI synthesis through the CDP-diacylglycerol pathway (Hermansson et al., 2011). We tested the activity of PAP-2/LPPs and PAP-1/lipin in the liver and after differentiating them in terms of their dependence on  $Mg^{2+}$  and sensitivity to NEM, under this assay condition only PAP-1 activity was observed. Based on this finding, we focused our attention on the temporal regulation of PAP-1/lipin activity in relation to its role in GPL biosynthesis. Overall, the activity of both enzymes (LPAAT and PAP-1/lipin) in the mouse liver displayed a similar daily fluctuation under both LD and DD. Strikingly, the lowest levels of PAP-1/lipin activity were recorded around 20 h post-synchronization, the time at which LPAAT also showed the lowest activity, most likely in order to keep PA levels constant. Both enzymes present the highest levels of activity during the day or at the day/night transition (dusk). At these phases, PA is metabolized to DAG rather than being accumulated. The resulting higher DAG content could be transiently utilized for the *de novo* synthesis of GPLs during these phases, though the possibility that elevated PA content is necessary for PI synthesis and/or other intracellular functions such as cell signaling cannot be discarded. In addition, and in further support of our observations, a recent report has demonstrated that the transcripts for the enzymes of the glycerol-3-phosphate pathway (LPLAT, PAP-1/lipin, etc.) are also expressed in a circadian manner (Adamovich et al., 2014).

The generation of LPA is the result of the esterification of glycerol-3-phosphate whereas other lysophospholipids are formed by the action of phospholipase A (PLA) activities as part of the deacylation-reacylation cycle (Shindou et al., 2009). For this reason LPLATs may reflect the state of the GPL deacylation/reacylation cycle, and the possibility of a differential temporal regulation of PLA cannot be discarded. Indeed, the LPLAT activities of the different lysophospholipids examined (LPC, LPE and LPI) presented similar circadian patterns, mostly with highest levels at 16 h during the early subjective night and during a time window around 32 h (28, 32 and 40 h) with a clear delay with respect to PAP-1/lipin activity and the endogenous content of main GPLs. The temporal variations observed in LPLAT activities may generate significant variations

in the fatty acid composition and quality of GPLs, affecting the membrane curvature and fluidity and ultimately regulating the activity and function of different cellular processes (Shindou & Shimizu, 2009). Our observations clearly show that the *de novo* biosynthesis and remodeling of GPLs are subjected to endogenous temporal control in the liver of mouse, likely reflecting differential requirements over time of newly synthesized phospholipids for membrane biogenesis and/or generation of second lipid messenger waves. In addition, our findings may suggest that the temporal separation of events within the cell also contributes to the spatial organization of reactions in the different cell compartments. The biogenesis of new membrane is required for a number of cellular processes, including cell proliferation in tissue regeneration, exocytosis, vesicular traffic, organelle formation, etc. The metabolic oscillations described may, among other roles, represent a general characteristic of oscillators present either in the mouse liver, in immortalized cell cultures (NIH 3T3) or neuronal cells (Acosta-Rodríguez et al., 2013; Adamovich et al., 2014; Garbarino-Pico et al., 2004; Guido et al., 2001).

Of all individual GPLs examined in this paper, we have paid particular attention to PC metabolism, seeking to determine its endogenous levels, the activity of LPCAT and the expression of its synthesizing enzymes, ChoK and CCT, from the Kennedy pathway and also of PEMT, an enzyme which plays a key role in the alternative liver route of PC synthesis. PC homeostasis in the liver is regulated at multiple levels. 70% of PC is biosynthesized from choline via the CDP-choline pathway and 30% is derived from PE via the PEMT pathway (Leonardi et al., 2009; Vance, 2002). Lipoproteins (HDL and LDL) transport PC into the liver, while PC provides choline for sphingomyelin synthesis and is also a precursor of PS. A major loss of hepatic PC occurs from biliary secretion. In addition to the degradation of PC by phospholipases, hepatic PC can also be secreted as an important component of very low-density (VLDL) and high-density (HDL) lipoproteins. We demonstrate here that mouse liver GPL metabolism oscillates rhythmically with a precise temporal control. Taking into account that our findings are reported using an *in vivo* experimental model we cannot discard the possibility that the mentioned mechanisms oscillate rhythmically and in consequence regulate liver PC content and the PC/PE ratio. In addition, as our experimental design involved whole hepatic homogenates, we cannot discard that diurnal variations may take place in the size and proportion of liver organelles involved in lipid synthesis as previously described (Chedid & Nair, 1972; Uchiyama et al., 1981) as well as in levels of S-adenosylmethionine and S-adenosylhomocysteine (Chagoya de Sánchez et al., 1991) to further contribute to changes in the PC/PE ratio. Although multiple levels of control may act to temporally regulate the metabolism of PC in the murine

liver, the activation of specific key regulatory synthesizing enzymes at the level of expression and/or activity may differentially contribute at particular times after LD synchronization.

The variations observed in the endogenous content of PC in the mouse liver may be due at least in part to a number of possibilities, such as a higher availability of DAG differentially generated by PAP-1/lipin during the day, an increase in PC production by LPCAT activity at early subjective night or at dusk and/or concerted changes in mRNA levels of the regulatory enzymes ChoK and PEMT. In fact, the expression of both *ChoK $\alpha$*  and PEMT mRNAs exhibited a significant daily variation in the synchronized livers with highest levels during subjective night in DD and the lowest values during the projected day. Strikingly, ChoK has been shown to be strongly expressed in tumor cells (Gallego-Ortega et al., 2011) and although this enzyme is not the rate-limiting enzyme in PC synthesis, it has been proposed to function as a key regulatory enzyme (Araki & Wurtman, 1998; Infante & Kinsella, 1978; Kent, 2005; Marcucci et al., 2010) which seems to be tightly regulated in a circadian manner. By contrast, no circadian variations were seen in levels of CCT mRNA isoforms (data not shown), which is the rate-limiting enzyme. Although CPT has not been shown to be a regulatory or rate-limiting enzyme in PC synthesis (Infante, 1977), we cannot discard variations in its levels of expression and/or activity over time.

Our findings suggest that both ChoK and PEMT, at least at the mRNA level, may temporally contribute to the regulation of PC biosynthesis in the liver. It is interesting to note that the alternative PC biosynthetic pathway, involving PEMT to catalyze the formation of PC from PE (Li & Vance, 2008) and reported to be of great importance in the liver, displayed higher levels of expression at night, at times at which nocturnal animals are fully active. Apart from the clock regulation, PC metabolism may also be regulated by homeostatic mechanisms, such as substrate availability, the state of enzyme activities (post-translational modifications and subcellular localization), the presence of specific regulatory factor, and rate-limiting steps, among others (Araki & Wurtman, 1998; Coleman & Mashek, 2011; Hermansson et al., 2011; Kent, 2005). Although in our experimental protocol animals were fed *ad libitum*, since they have nocturnal habits, the highest concentration of available nutrients and substrates are obtained during the dark phase of the LD cycle or the subjective night; in fact, animals eat around 80% of total daily food during the night. Moreover, timed restricted feeding (RF) might provide a time cue and reset the circadian clock in the liver and other organs, leading to better health (Adamovich et al., 2014; Sherman et al., 2012; Vollmers et al., 2009). In addition, changes in catabolic and anabolic pathways were reported to alter liver metabolome and improve nutrient utilization and energy expenditure (Hatori et al., 2012). Circadian

clocks located in the liver and other organs and tissues can drive a series of physiological functions including those relating to lipid metabolism (Asher & Schibler, 2011; Bass & Takahashi, 2010; Bray & Young, 2011; Eckel-Mahan et al., 2012), in all likelihood regardless of food availability; however, the timing of food availability can alter the phases of the oscillations. The disruption of the circadian molecular clock may result in a number of metabolic disorders including obesity and diabetes (Durgan & Young, 2010; Froy, 2010; Green et al., 2008; Maury et al., 2010; Sookoian et al., 2008; Takahashi et al., 2008).

Overall, our observations lead us to infer that the biosynthesis of whole GPLs and particularly of PC in the mammalian liver undergoes clear temporal variations, somehow sensing the time of day in relation to external cues (food, temperature, hormones, etc.). The circadian regulation of GPL content may be crucial to the temporal organization of a number of cellular processes such as membrane renewal and fluidity, vesicular trafficking, exocytosis, membrane protein activity (receptors, channels, etc.), second messenger reservoir changes and/or cell proliferation under homeostatic levels or regenerating conditions.

## ACKNOWLEDGMENTS

The authors thank Dr Daniela Bussolino for her excellent technical support and collaboration.

## DECLARATION OF INTEREST

The authors report no conflicts of interest.

This work was supported by Agencia Nacional de Promoción Científica y Tecnológica (FONCyT) (PICT 2004 N° 967, PICT 2006 N° 898 and PICT 2010 N° 647), Secretaría de Ciencia y Técnica-Universidad Nacional de Córdoba (SeCyT-UNC), Consejo Nacional de Investigaciones Científicas y Tecnológicas de Argentina (CONICET), Ministerio de Ciencia y Técnica de Córdoba, Fundación Antorchas and Florencio Fiorini.

## REFERENCES

- Abe M, Herzog E, Yamazaki S, et al. (2002). Circadian rhythms in isolated brain regions. *J Neurosci.* 22:350–6.
- Acosta-Rodríguez V, Márquez S, Salvador G, et al. (2013). Daily rhythms of glycerophospholipid synthesis in fibroblast cultures involve differential enzyme contributions. *J Lipid Res.* 54: 1798–811.
- Adamovich Y, Rousso-Noori L, Zwihaft Z, et al. (2014). Circadian clocks and feeding time regulate the oscillations and levels of hepatic triglycerides. *Cell Metab.* 19:319–30.
- Aoyama C, Liao H, Ishidate K. (2004). Structure and function of choline kinase isoforms in mammalian cells. *Prog Lipid Res.* 43: 266–81.
- Araki W, Wurtman RJ. (1998). How is membrane phospholipid biosynthesis controlled in neural tissues? *J Neurosci Res.* 51: 667–74.

- Asher G, Schibler U. (2011). Crosstalk between components of circadian and metabolic cycles in mammals. *Cell Metab.* 13: 125–37.
- Balsalobre A, Damiola F, Schibler U. (1998). A serum shock induces circadian gene expression in mammalian tissue culture cells. *Cell.* 93:929–37.
- Bass J, Takahashi JS. (2010). Circadian integration of metabolism and energetics. *Science.* 330:1349–54.
- Bradford MM. (1976). A rapid and sensitive method for the quantitation of microgram quantities of protein utilizing the principle of protein-dye binding. *Analyt Biochem.* 72:248–54.
- Bray M, Young ME. (2011). Regulation of fatty acid metabolism by cell autonomous circadian clocks: Time to fatten up on information? *J Biol Chem.* 286:11883–9.
- Brindley DN. (2004). Lipid phosphate phosphatases and related proteins: Signaling functions in development, cell division, and cancer. *J Cell Biochem.* 92:900–12.
- Castagnet PI, Giusto NM. (2002). Effect of light and protein phosphorylation on photoreceptor rod outer segment acyltransferase activity. *Arch Biochem Biophys.* 403:83–91.
- Chagoya de Sánchez V, Hernández-Muñoz R, Sánchez L, et al. (1991). Twenty-four-hour changes of S-adenosylmethionine, S-adenosylhomocysteine adenosine and their metabolizing enzymes in rat liver; possible physiological significance in phospholipid methylation. *Int J Biochem.* 23:1439–43.
- Chedid A, Nair V. (1972). Diurnal rhythm in endoplasmic reticulum of rat liver: Electron microscopic study. *Science.* 175:176–9.
- Churchward MA, Brandman DM, Rogasevskaia T, Coorsen JR. (2008a). Copper (II) sulfate charring for high sensitivity on-plate fluorescent detection of lipids and sterols: Quantitative analyses of the composition of functional secretory vesicles. *J Chem Biol.* 1:79–87.
- Churchward MA, Rogasevskaia T, Brandman DM, et al. (2008b). Specific lipids supply critical negative spontaneous curvature – an essential component of native Ca(2+)-triggered membrane fusion. *Biophys J.* 94:3976–86.
- Coleman RA, Mashek DG. (2011). Mammalian triacylglycerol metabolism: Synthesis, lipolysis, and signaling. *Chem Rev.* 111:6359–86.
- Csaki LS, Dwyer JR, Fong LG, et al. (2013). Lipins, lipinopathies, and the modulation of cellular lipid storage and signaling. *Prog Lipid Res.* 52:305–16.
- Cui Z, Houweling M. (2002). Phosphatidylcholine and cell death. *Biochim Biophys Acta.* 1585:87–96.
- de Arriba Zerpa GA, Guido ME, Bussolino DF, et al. (1999). Light exposure activates retina ganglion cell lysophosphatidic acid acyl transferase and phosphatidic acid phosphatase by a c-fos-dependent mechanism. *J Neurochem.* 73:1228–35.
- Díaz-Muñoz M, Suárez J, Hernández-Muñoz R, et al. (1987). Day-night cycle of lipidic composition in rat cerebral cortex. *Neurochem Res.* 12:315–21.
- Donkor J, Sariahmetoglu M, Dewald J, et al. (2007). Three mammalian lipins act as phosphatidate phosphatases with distinct tissue expression patterns. *J Biol Chem.* 282:3450–7.
- Dunlap JC, Loros JJ, DeCoursey PJ. (2004). *Chronobiology. Biological timekeeping.* Sunderland, MA: SINAUER edition.
- Durgan DJ, Young ME. (2010). The cardiomyocyte circadian clock: Emerging roles in health and disease. *Circ Res.* 106:647–58.
- Eckel-Mahan KL, Patel VR, Mohny RP, et al. (2012). Coordination of the transcriptome and metabolome by the circadian clock. *Proc Natl Acad Sci USA.* 109:5541–6.
- Exton JH. (1994). Phosphatidylcholine breakdown and signal transduction. *Biochim Biophys Acta.* 1212:26–42.
- Fine JB, Sprecher H. (1982). Unidimensional thin-layer chromatography of phospholipids on boric acid-impregnated plates. *J Lipid Res.* 23:660–3.
- Folch J, Lees M, Stanley Sloane GH. (1957). A simple method for the isolation and purification of total lipides from animal tissues. *J Biol Chem.* 226:497–509.
- Froy O. (2010). Metabolism and circadian rhythms – Implications for obesity. *Endocrine Rev.* 31:1–24.
- Gallego-Ortega D, Gómez del Pulgar T, Valdés-Mora F, et al. (2011). Involvement of human choline kinase alpha and beta in carcinogenesis: A different role in lipid metabolism and biological functions. *Adv Enzyme Reg.* 51:183–94.
- Garbarino-Pico E, Carpentieri AR, Castagnet PI, et al. (2004). Synthesis of retinal ganglion cell phospholipids is under control of an endogenous circadian clock: Daily variations in phospholipid-synthesizing enzyme activities. *J Neurosci Res.* 76:642–52.
- Garbarino-Pico E, Valdez DJ, Contin MA, et al. (2005). Rhythms of glycerophospholipid synthesis in retinal inner nuclear layer cells. *Neurochem Int.* 47:260–70.
- Gehrig K, Cornell RB, Ridgway ND. (2008). Expansion of the nucleoplasmic reticulum requires the coordinated activity of lamins and CTP: Phosphocholine cytidylyltransferase alpha. *Molec Biol Cell.* 19:237–47.
- Ginovker A, Zhikhareva A. (1982). Circadian rhythm of liver phospholipids in normal hamsters and hamsters with opisthorchiasis. *Bull Exp Biol Med.* 94:45–8.
- Giusto NM, Bazan N. (1979). Phospholipids and acylglycerols biosynthesis and <sup>14</sup>CO<sub>2</sub> production from [<sup>14</sup>C]glycerol in the bovine retina: The effects of incubation time, oxygen and glucose. *Exp Eye Res.* 29:155–68.
- Giusto NM, Pasquare SJ, Salvador GA, et al. (2000). Lipid metabolism in vertebrate retinal rod outer segments. *Prog Lipid Res.* 39:315–91.
- Giusto NM, Pasquare SJ, Salvador GA, Ilincheta de Boschero MG. (2010). Lipid second messengers and related enzymes in vertebrate rod outer segments. *J Lipid Res.* 51:685–700.
- Giusto NM, Salvador GA, Castagnet PI, et al. (2002). Age-associated changes in central nervous system glycerolipid composition and metabolism. *Neurochem Res.* 27:1513–23.
- Glunde K, Bhujwala ZM, Ronen SM. (2011). Choline metabolism in malignant transformation. *Nat Rev Cancer.* 11:835–48.
- Green CB, Takahashi JS, Bass J. (2008). The meter of metabolism. *Cell.* 134:728–42.
- Guido ME, Garbarino-Pico E, Caputto BL. (2001). Circadian regulation of phospholipid metabolism in retinal photoreceptors and ganglion cells. *J Neurochem.* 76:835–45.
- Hatori M, Vollmers C, Zarrinpar A, et al. (2012). Time-restricted feeding without reducing caloric intake prevents metabolic diseases in mice fed a high-fat diet. *Cell Metab.* 15:848–60.
- Hermansson M, Hokynar K, Somerharju P. (2011). Mechanisms of glycerophospholipid homeostasis in mammalian cells. *Prog Lipid Res.* 50:240–57.
- Huang W, Ramsey KM, Marcheva B, Bass J. (2011). Circadian rhythms, sleep, and metabolism. *J Clin Invest.* 121:2133–41.
- Hughes M, DiTacchio L, Hayes K, Vollmers C. (2009). Harmonics of circadian gene transcription in mammals. *PLoS Genet.* 5: e1000442.
- Infante JP, Kinsella JE. (1978). Control of phosphatidylcholine synthesis and the regulatory role of choline kinase in rat liver. Evidence from essential-fatty acid-deficient rats. *Biochem J.* 176:631–3.
- Infante JP. (1977). Rate-limiting steps in the cytidine pathway for the synthesis of phosphatidylcholine and phosphatidylethanolamine. *Biochem J.* 167:847–9.
- Karim MA, Jackson P, Jackowski S. (2003). Gene structure, expression and identification of a new CTP: Phosphocholine cytidylyltransferase [beta] isoform. *Biochim Biophys Acta (BBA).* 1633:1–12.
- Kennedy EP, Weiss SB. (1956). The function of cytidine coenzymes in the biosynthesis of phospholipides. *J Biol Chem.* 222: 193–214.
- Kent C. (2005). Regulatory enzymes of phosphatidylcholine biosynthesis: A personal perspective. *Biochim Biophys Acta (BBA).* 1733:53–66.

- Kok BP, Venkatraman G, Capatos D, Brindley DN. (2012). Unlike two peas in a pod: Lipid phosphate phosphatases and phosphatidate phosphatases. *Chem Rev.* 112:5121–46.
- Kornmann B, Schaad O, Bujard H, et al. (2007). System-driven and oscillator-dependent circadian transcription in mice with a conditionally active liver clock. *PLoS Biol.* 5:e34.
- Larionov A, Krause A, Miller W. (2005). A standard curve based method for relative real time PCR data processing. *BMC Bioinform.* 6:62–78.
- Leonardi R, Frank MW, Jackson PD, et al. (2009). Elimination of the CDP-ethanolamine pathway disrupts hepatic lipid homeostasis. *J Biol Chem.* 284:27077–89.
- Li Z, Agellon LB, Allen TM, et al. (2006). The ratio of phosphatidylcholine to phosphatidylethanolamine influences membrane integrity and steatohepatitis. *Cell Metab.* 3:321–31.
- Li Z, Vance DE. (2008). Phosphatidylcholine and choline homeostasis. *J Lipid Res.* 49:1187–94.
- Livak KJ, Schmittgen TD. (2001). Analysis of relative gene expression data using real-time quantitative PCR and the 2<sup>-</sup>[Delta][Delta] CT method. *Methods.* 25:402–8.
- Marcucci H, Paoletti L, Jackowski S, Banchio C. (2010). Phosphatidylcholine biosynthesis during neuronal differentiation and its role in cell fate determination. *J Biol Chem.* 285: 25382–93.
- Mardia KV. (1976). Linear-circular correlation coefficients and rhythmometry. *Biometrika.* 63:403–5.
- Marquez S, Crespo P, Carlini V, et al. (2004). The metabolism of phospholipids oscillates rhythmically in cultures of fibroblasts and is regulated by the clock protein PERIOD 1. *FASEB J.* 18: 519–21.
- Matsuo T, Yamaguchi S, Mitsui S, et al. (2003). Control mechanism of the circadian clock for timing of cell division in vivo. *Science.* 302:255–9.
- Maury E, Ramsey KM, Bass J. (2010). Circadian rhythms and metabolic syndrome from experimental genetics to human disease. *Circ Res.* 106:447–62.
- Menger GJ, Allen GC, Neuendorff N, et al. (2007). Circadian profiling of the transcriptome in NIH/3T3 fibroblasts: Comparison with rhythmic gene expression in SCN2. 2 cells and the rat SCN. *Physiol Genom.* 29:280–9.
- Mohawk JA, Green CB, Takahashi JS. (2012). Central and peripheral circadian clocks in mammals. *Ann Rev Neurosci.* 35:445–62.
- Nagoshi E, Brown SA, Dibner C, et al. (2005). Circadian gene expression in cultured cells. *Meth Enzymol.* 393:543–57.
- Panda S, Antoch MP, Miller BH, et al. (2002). Coordinated transcription of key pathways in the mouse by the circadian clock. *Cell.* 109:307–20.
- Pascual F, Carman GM. (2013). Phosphatidate phosphatase, a key regulator of lipid homeostasis. *Biochim Biophys Acta (BBA) – Mol Cell Biol Lipids.* 1831:514–22.
- Pasquare de Garcia SJ, Giusto NM. (1986). Phosphatidate phosphatase activity in isolated rod outer segment from bovine retina. *Biochim Biophys Acta.* 875:195–202.
- Pasquare SJ, Giusto NM. (1993). Differential properties of phosphatidate phosphohydrolase and diacylglyceride lipase activities in retinal subcellular fractions and rod outer segments. *Compar Biochem Physiol Part B.* 104:141–8.
- Pasquare SJ, Salvador GA, Giusto NM. (2004). Phospholipase D and phosphatidate phosphohydrolase activities in rat cerebellum during aging. *Lipids.* 39:553–60.
- Portaluppi F, Smolensky MH, Touitou Y. (2010). Ethics and methods for biological rhythm research on animals and human beings. *Chronobiol Int.* 27:1911–29.
- Ramírez de Molina A, Rodríguez-González A, Gutiérrez R, et al. (2002). Overexpression of choline kinase is a frequent feature in human tumor-derived cell lines and in lung, prostate, and colorectal human cancers. *Biochem Biophys Res Commun.* 296: 580–3.
- Reddy AB, Karp NA, Maywood ES, et al. (2006). Circadian orchestration of the hepatic proteome. *Curr Biol.* 16:1107–15.
- Reue K, Brindley DN. (2008). Thematic review series: Glycerolipids. Multiple roles for lipins/phosphatidate phosphatase enzymes in lipid metabolism. *J Lipid Res.* 49:2493–503.
- Sahar S, Sassone-Corsi P. (2012). Regulation of metabolism: The circadian clock dictates the time. *Trends Endocrinol Metab.* 23: 1–8.
- Sen A, Hui SW. (1988). Direct measurement of headgroup hydration of polar lipids in inverted micelles. *Chem Phys Lipids.* 49: 179–84.
- Sherman H, Genzer Y, Cohen R, et al. (2012). Timed high-fat diet resets circadian metabolism and prevents obesity. *FASEB J.* 26: 3493–502.
- Shindou H, Hishikawa D, Harayama T, et al. (2009). Recent progress on acyl CoA: Lysophospholipid acyltransferase research. *J Lipid Res* 50:S46–51.
- Shindou H, Shimizu T. (2009). Acyl-CoA: Lysophospholipid acyltransferases. *J Biol Chem.* 284:1–5.
- Sleight R, Kent C. (1983). Regulation of phosphatidylcholine biosynthesis in mammalian cells. II. Effects of phospholipase C treatment on the activity and subcellular distribution of CTP: Phosphocholine cytidyltransferase in Chinese hamster ovary and LM cell lines. *J Biol Chem.* 258:831–5.
- Sookoian S, Gemma C, Gianotti TF, et al. (2008). Genetic variants of clock transcription factor are associated with individual susceptibility to obesity. *Am J Clin Nutr.* 87:1606–15.
- Takahashi JS, Hong HK, Ko CH, McDearmon EL. (2008). The genetics of mammalian circadian order and disorder: Implications for physiology and disease. *Nat Rev Genet.* 9: 764–75.
- Turek FW, Joshu C, Kohsaka A, et al. (2005). Obesity and metabolic syndrome in circadian clock mutant mice. *Science.* 308:1043–5.
- Uchiyama Y, Groh V, von Mayersbach H. (1981). Different circadian variations as an indicator of heterogeneity of liver lysosomes. *Histochemistry.* 73:321–37.
- Van Meer G, Voelker DR, Feigenson GW. (2008). Membrane lipids: Where they are and how they behave. *Nat Rev Mol Cell Biol.* 9: 112–24.
- Vance DE, Vance JE. (2009). Physiological consequences of disruption of mammalian phospholipid biosynthetic genes. *J Lipid Res.* 50:S132–7.
- Vance DE. (2002). Phospholipid biosynthesis in eukaryotes. *New Comprehensive Biochem.* 36:205–32.
- Vollmers C, Gill S, DiTacchio L, et al. (2009). Time of feeding and the intrinsic circadian clock drive rhythms in hepatic gene expression. *Proc Natl Acad Sci USA.* 106:21453–8.
- Weinhold PA, Charles L, Rounsifer ME, et al. (1991). Control of phosphatidylcholine synthesis in Hep G2 cells, effect of fatty acids on the activity and immunoreactive content of choline phosphate cytidyltransferase. *J Biol Chem.* 266: 6093–100.
- Weinhold PA, Rethy VB. (1974). The separation, purification, and characterization of ethanolamine kinase and choline kinase from rat liver. *Biochemistry.* 13:5135–41.
- Wu G, Vance DE. (2010). Choline kinase and its function. *Biochem Cell Biol.* 88:559–64.

### Supplementary material available online

#### Supplementary Table 1 and Figure 1